Received 24 May 2023; accepted 28 May 2023. Date of publication 1 June 2023; date of current version 12 June 2023.
The review of this article was arranged by Editor Z. Zhang.

Digital Object Identifier 10.1109/JEDS.2023.3281866

Review: Numerical Simulations of Semiconductor Piezoresistance for Computer-Aided Designs

TAKAYA SUGIURA [1] (Member, IEEE), KAZUNORI MATSUDA [2], AND NOBUHIKO NAKANO [1] (Member, IEEE)

1 Department of Electronics and Electrical Engineering, Keio University, Yokohama 223-8522, Kanagawa, Japan
2 Division of Electrical, Electronic and Infocommunications Engineering, Graduate School of Engineering, Osaka University, Suita 565-0871, Osaka, Japan

CORRESPONDING AUTHOR: T. SUGIURA (e-mail: takaya_sugiura@ieee.org)

ABSTRACT The field of piezoresistance has mainly advanced through experimental research; however, the improved accuracy of simulations and the emergence of new materials have increased the importance of simulations in this field. This review discusses the methods and current topics related to simulations of piezoresistive devices. Advancing simulation modeling will facilitate the computer-aided design of piezoresistive devices, and this review introduces the means of establishing these models by discussing the current studies on simulations and calculations in this field. Two simulation methods currently exist namely, device simulations and first-principles theoretical analysis. This review focuses on numerical simulation approaches for modeling of the piezoresistive effect using the multiphysics simulations of the mechanical and electrical behaviors of piezoresistive materials.

INDEX TERMS Semiconductor piezoresistance, computer-aided design.

I. INTRODUCTION

Piezoresistance is the main principle of mechanical sensing because it provides good linearity and high sensitivity. Owing to these advantages, the piezoresistive sensing element is the major component of the pressure sensors in micro-electro-mechanical-systems (MEMS) [2], [3], [4]. For piezoresistive sensing elements, the use of semiconductor materials is more advantageous than the use of metals because of the band-gap transformation feature of semiconductors, the physics of which is different from the electrical effect of metals [1]. Investigations of semiconductor-based piezoresistance require interdisciplinary approaches at the boundary between electronics and mechanical engineering [5]. Thus far, fundamental research on piezoresistance has been limited, and only several experimental studies for various applications in the field have been reported. Several reports are available on the gauge factor (GF) measurements of new materials such as wide band-gap semiconductors and improved sensor structures. Additionally, theoretical studies based on first-principles calculations have been conducted to obtain fundamental material properties by purely theoretical methods. The abovementioned studies are important for revealing material properties under stress; additionally, these modeling studies have been beneficial for device development by providing input information to the device simulations [6].

The topics currently under active research in this field include the study of new materials, with a particular focus on wide band-gap semiconductors that provide several advantages over the conventional silicon [7]. To date, material parameters and the fabrication of piezoresistive devices have been reported. Device simulations require the fundamental knowledge of material properties as inputs. Although the fundamental material properties have been sufficiently established, only a limited number of studies have focused on device simulation based on material properties. The reasons for this are as follows: 1) difficulty in establishing simulation models because these must consider the multiphysics of mechanical and electrical components, and 2) the corresponding physical models are still under investigation. A diverse range of piezoresistive devices are currently available, including piezoresistors, accelerometers, and enhanced-speed metal-oxide-semiconductor field-effect transistors (MOSFETs) using strained-silicon [8], [9], [10].

Thus, evaluating the piezoresistive effect for the design of these devices is important.

Herein, the current studies based on the numerical simulations of piezoresistance are reviewed. The remainder of the article introduces material properties and briefly introduces first-principle calculations (Section II), as well as the methods for piezoresistance evaluation and piezoresistance-based applications (Section III).

II. PHYSICS OF PIEZORESISTANCE

A. FUNDAMENTAL PHYSICS

The piezoresistive effect is expressed using the piezoresistive coefficient π (unit Pa^{-1}), which is unique for each material. The coefficients in the longitudinal (parallel to the current flow) and transverse (normal to the current flow) directions must be considered. Using the applied stresses σ_l for each direction, the piezoresistance is expressed as

$$\frac{\Delta R}{R_0} = \pi_l \sigma_l + \pi_t \sigma_t. \tag{1}$$

Additionally, GF is the sensitivity of the resistance change, which is defined as the ratio of the resistance change and strain ε as follows:

$$GF = \frac{\Delta R}{\varepsilon R_0} = \frac{\pi_l \sigma_l + \pi_t \sigma_t}{\varepsilon}. \tag{2}$$

This expression indicates that the change in the resistance of the material is proportional to the strain ε with a slope GF; therefore, good linearity, which is important for sensing, can be ensured.

The piezoresistive coefficient is expressed as a 6×6 tensor. By symmetry, the final components are π_{11}, π_{12}, and π_{44} for cubic crystals and π_{22} and π_{33} for hexagonal crystals. The longitudinal and transverse piezoresistive coefficients are calculated using the orientation of the crystal [11], and are considered to be the effective piezoresistive coefficients. Furthermore, GF can be expressed using Young's modulus E (Pa), which is the stress under a unit strain [12].

$$GF = \pi E \tag{3}$$

Cantilever [13] and membrane [14] structures are widely used for implementing piezoresistive sensors. The cantilever and membrane structures are considered to be one-dimensional and two-dimensional structures, respectively (Fig. 1). This difference in dimensionality leads to different issues in the simulations of these structures; the one-dimensional cantilever structure is suitable for material property evaluations owing to its fewer-dimensional stress profile, and the two-dimensional membrane structure is used for optimizing the device structure. Reproducibility has been reported to be more challenging for the cantilever structure than for the membrane structure [15]; this was attributed to the effect of asymmetry of the cantilever structure. Nevertheless, currently, cantilever-based devices are the mainstream devices for academic research on piezoresistive sensor materials. Although piezoresistors show high sensitivity, the absolute output is small and a Wheatstone bridge circuit is used to detect small changes in the resistance of piezoresistors.

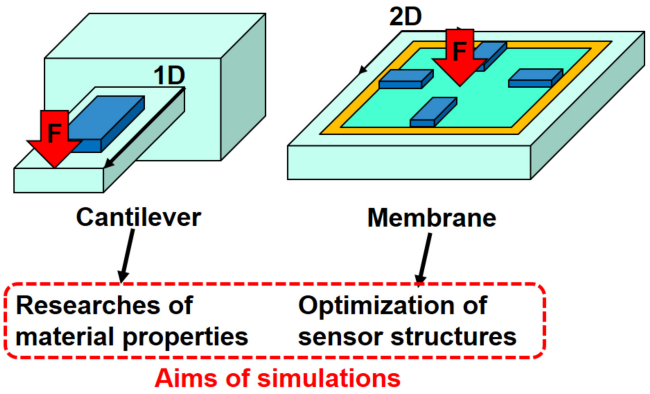

FIGURE 1. Structures of piezoresistors and their dimensions and the goals of their simulations.

B. MATERIALS UNDER PIEZORESISTANCE

B.1. NARROW BAND-GAP SEMICONDUCTORS

The band deformation in semiconductors caused by strain was observed in 1950, and is the origin of semiconductor piezoresistance [17]. Subsequently, the first study on semiconductor piezoresistance was conducted in 1954 using germanium and silicon [16]. Fundamental piezoresistive coefficients have been reported for different doping types and resistivities that demonstrated the phenomenon in semiconductor materials. The values of these coefficients are much higher than those for the new wide band-gap semiconductor materials. This is related to the band-gap energy, i.e., the transformation of the band-gap structure can be large in the narrow band-gap silicon and germanium semiconductors. The temperature and doping-dependent piezoresistive coefficients in p-type silicon have been extensively studied by Richter et al. [18] in the temperature range of 200–450 K in which silicon is expected to operate. Matsuda et al. reported that the transfer of holes between the valence bands, as well as the stress-dependent effective mass, are crucial in the high-temperature region for p-type silicon [19]. This is also true for n-type silicon, in which the effective mass plays an important role [20]. Furthermore, p- and n-type Ge show high values of theoretical and experimental π_{44} piezoresistive coefficients [21]. Recently, Matsuda et al. reported that stress-dependent hole effective masses of light and heavy holes play key roles in the origin of the piezoresistive effect in p-type silicon materials [22].

Figure 2 presents an overview of piezoresistance for the conventional narrow band-gap and new wide band-gap materials. The main advantage of wide band-gap materials is their expanded range of applications such as applications in high-temperature and chemically corrosive environments, as well as in the presence of strong mechanical shocks. Some examples are the sensors on vehicles, airplanes, and gas turbines [7]. Although these materials possess relatively low GFs compared to that of Si, their excellent material

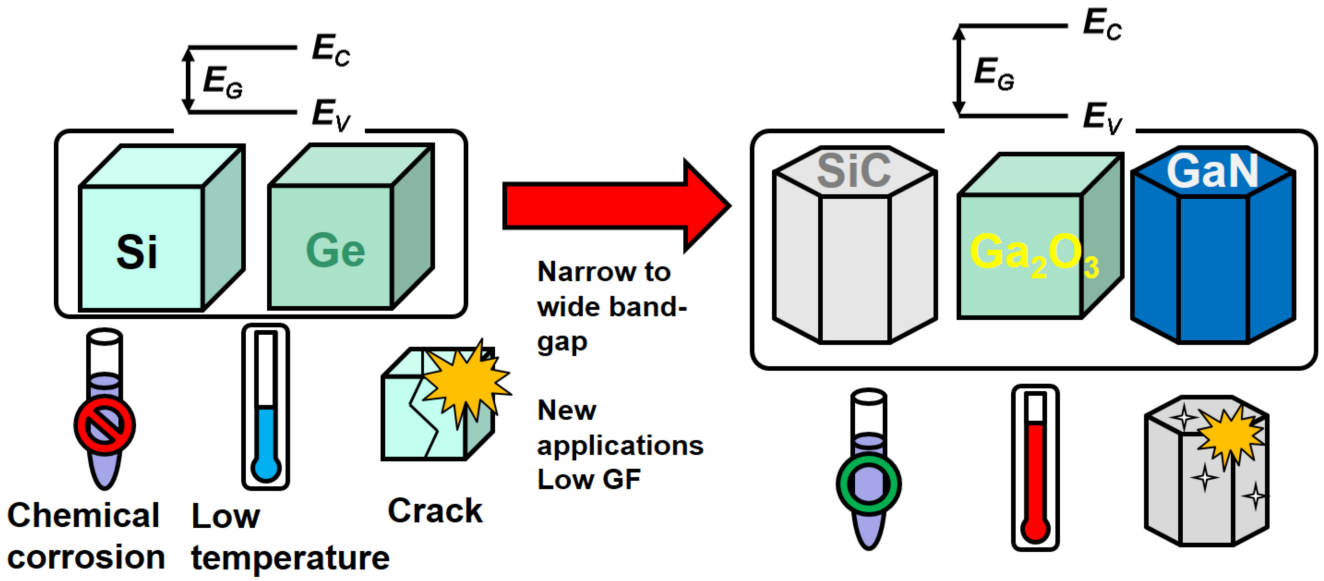

FIGURE 2. Illustrations of piezoresistance materials for the conventional and novel semiconductors.

properties enable their use in applications that are otherwise difficult to achieve using conventional silicon.

B.2. SILICON CARBIDES

Silicon carbides are the most popular wide band-gap semiconductors. Silicon carbide, including its different polytypes, has been extensively studied. The most common SiC is 3C-SiC, which has a cubic crystal structure. The fundamental piezoresistive coefficients have been reported for p- [23], [24] and n-type [25] silicon carbide. Additionally, the temperature effect has been studied from a low temperature of 150 K [26] to a high temperature of 723 K [25], [27], demonstrating the wide temperature range of piezoresistive silicon carbide applications.

The piezoresistive coefficients of p-type 4H-SiC were reported in 2018 for the π_{11} and π_{12} tensor components [28]. In 2022, these coefficients were reported for n-type materials [29], and (0001) plane evaluations can now be performed. The silicon carbide piezoresistors were formed on a silicon substrate using heterojunction technology, and a strong leakage-current inhibition was achieved [30]. The temperature robustness until 600 °C was demonstrated with a GF decrease of approximately 30% from the GF at room temperature. The reported GF value of 32 at room temperature for 4H-SiC is one of the highest among the reported values for wide band-gap materials, and the temperature robustness is also the highest, indicating that 4H-SiC may have potential for new applications.

Another type of hexagonal crystal, namely, 6H-SiC, has received less attention. Its longitudinal piezoresistive coefficient has been reported in several studies [31]; however, a range of values has been reported and therefore this coefficient is still considered to be undetermined. Therefore, we proposed a linear correction factor [34] to minimize GF measurement errors. Another approach determined the π_{11} and π_{12} piezoresistive coefficients [32] from the experimental results for n-type 6H-SiC piezoresistor operation [33].

B.3. GALLIUM NITRIDES

Studies on gallium nitride materials have been fewer compared to those on silicon carbides, and the piezoelectric properties of gallium nitride have been attributed to its III-V compound structure [35]. A large GF of 130 was reported in n-type gallium nitride due to a combination of the piezoresistive and piezoelectric phenomena [36]. The temperature robustness up to 125 °C was reported by observing the high-temperature stability of the GF value [37]. Although the piezoresistive coefficients of this material have not been studied well, its longitudinal piezoresistive coefficient π_{11} was reported as $\pi_{11} = 9.4 \times 10^{-11}$ Pa^{-1} [32].

B.4. OTHER MATERIALS

Gallium (III) oxide is a wide band-gap semiconductor, and its piezoresistance was first demonstrated in 2019 [38]. Subsequently, the piezoresistive coefficient of this material was reported in 2021, which is $\pi_{11} = -1.2 \times 10^{-11}$ Pa^{-1} for the n-type material [39]. Other materials that experimentally exhibit relatively high sensitivities have also been reported, such as titanium dioxide [40], gallium arsenide [41], and zinc oxide [42]. Diamond exhibits piezoresistive effect in its single crystalline form [43], and its outstanding material characteristics make it suitable for sensing in harsh environments [44]. It has been reported that the concentration of the boron dopant determines the magnitude and sensitivity of diamond, particularly for its single-crystal form.

B.5. NANOWIRES

Nano-wire structures have been reported for several materials. A notable characteristic of nanowires is their large

piezoresistance; the piezoresistive coefficients of silicon and silicon carbide nanowires are on the order of 10^3 ($\times 10^{-11}$ Pa^{-1}) and 10^2, respectively [45], [46]. The detailed mechanism of piezoresistance in nanowires is presently under study, and one possible mechanism is the appearance of quantum confinement in nano-scale structures [48]. Barwicz et al. reported the structural characteristics of the piezoresistance of silicon nanowires. The width effect appeared under a thickness of 50 nm, which is expected to correspond to increased quantum effect [49]. Furthermore, the resistance of nanowires changes with time, and a significantly high resistance is obtained just after its solvent clean, which reveals its instability against the environment. Fakhri et al. compared the small compressive pressured piezoresistance between silicon nanowires and bulk silicon [47] and demonstrated the high sensitivity of nanowires to small pressure. Additionally, its piezoresistance is affected by hydrogenation: its sensitivity decreases drastically after hydrogenation, according to Barwicz's report [49]. The nanowire structure is an important sensing element in nano-microelectro-mechanical-systems [50], [51].

Thus far, almost all studies on nanowires have used silicon, and only a few studies have used other materials such as SiC. A very large GF value of -620.5 has been reported for boron-doped 3C-SiC nanowires; this value is substantially high compared to the values reported in previous studies on SiC nanowires [52]. Silicon nanowires are vulnerable to the stability of devices; therefore, using SiC may solve this problem because SiC is much stable against chemical reactions.

B.6. FLEXIBLE MATERIALS

Recently, flexible materials have attracted attention, and their piezoresistive characteristics are being studied intensively [53]. These materials are suitable for applications in brain–machine interfaces or bio-signal monitoring [54]. Li et al. categorized flexible piezoresistive sensors into three types, namely, conductive polymeric composites, porous conductive materials, and architected conductive materials. Most materials have been categorized as carbon materials (such as graphene and organic compounds) [55], [56], [57], and because flexible materials correspond to a small pressure (smaller than the order of kPa), their piezoresistive effects are more similar to structural changes in metals than to band deformation in semiconductors. Because the structures of flexible materials undergo deformation, the changes in structures must be considered. Graphene is expected to be the main material used for fabricating flexible materials, as it is a zero band-gap semiconductor [58] with large mechanical stiffness of 1 TPa, making it unique even among two-dimensional materials [59]. A simulation on flexible electronics using carbon nanotubes has been performed under small-pressure conditions [60]. Considering that mechanical effects are dominant in flexible electronics, structural analysis software using finite element methods will be highly suitable for analysing them.

TABLE 1. First-order piezoresistive coefficients of six piezoresistive tensor components for semiconductors (all units are [$\times 10^{-11}$ Pa^{-1}]).

Material	π_{11}	π_{12}	π_{22}	π_{33}	π_{44}
p-Si [16]	6.6	-1.1	-	-	138.1
n-Si [16]	-102.2	53.4	-	-	-13.6
p-Ge [16]	-10.6	5.0	-	-	88.6
n-Ge [16]	-5.2	-5.5	-	-	-138.7
p-SiC(3C) [24]	1.5	-1.4	-	-	18.1
n-SiC(3C) [25]	-9.6	5.8	-	-	1.6
p-SiC(4H) [28]	6.43	-5.12	N/A	N/A	N/A
n-SiC(4H) [29]	-3.4	6.15	N/A	N/A	N/A
n-SiC(6H) [32]	-4.8	3.1	N/A	N/A	N/A
n-GaN(H) [32]	9.4	N/A	N/A	N/A	N/A
n-$Ga_2O_3(\beta)$ [39]	-1.2	N/A	-	-	N/A
p-Diamond (SCD: low B/C) [43]	-0.21	0.13	-	-	3.85
p-Diamond (SCD: middle B/C) [43]	-0.68	0.72	-	-	3.27
p-Diamond (SCD: high B/C) [43]	0.3	0.08	-	-	2.36
p-Diamond (PCD) [43]	0.5	0.38	-	-	0.32

Furthermore, the fabrication of silicon LSI chips on flexible materials has been studied. Vilouras et al. fabricated a standard CMOS LSI chip on a flexible material and established the simulation modeling of transistors under tensile and compressive conditions [61].

B.7. SUMMARY

Table 1 summarizes the reported first-order fundamental piezoresistive coefficients of semiconductors. To date, research attention has been directed to cubic crystals, and common silicon, germanium, and 3C-SiC materials have been extensively studied. Fewer studies on hexagonal crystals have been reported compared to the studies on cubic crystals. Additionally, only the π_{11} and π_{12} coefficients have been reported.

C. FIRST-PRINCIPLES CALCULATIONS

To date, most theoretical research is based on first-principles calculations, which are beneficial for evaluating the physics of a material without any experimental data [62]. This method is suitable for obtaining material parameters such as piezoresistive coefficients. Furthermore, the complex physics governing applications can also be investigated using the values obtained by first-principles calculations. QuantumATK is a commercially available software package for first-principles calculations developed by Synopsys, Inc. Reference [63] that contains several Python programs [64].

For bulk materials, fundamental investigations of silicon piezoresistance have been performed using first-principle calculations [65]. Temperature dependences of piezoresistive coefficients with different doping concentrations can be expressed by the potential deformation of the conduction band [66] and the carrier distribution and transport modeled using effective masses. Different origins of the piezoresistive coefficients for different directions were observed; the longitudinal and transverse piezoresistive coefficients arise from the energy gap between valleys, and the shear piezoresistive

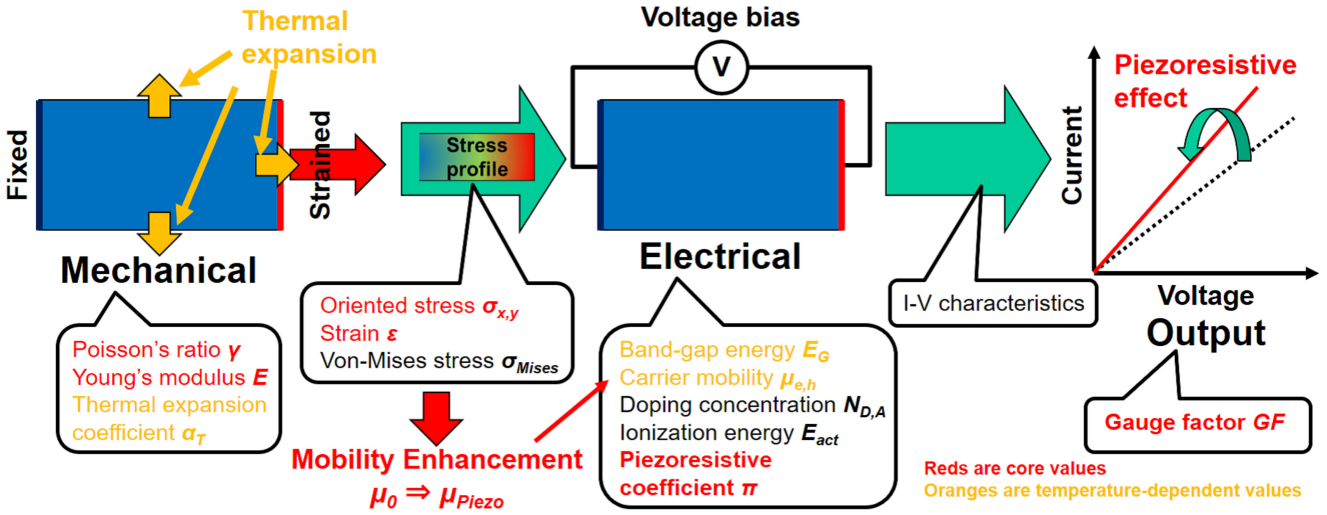

FIGURE 3. Basic simulation flow for studies on semiconductor piezoresistors.

coefficient arises from the distortion of the band energy surface.

For 3C-SiC, investigations of the dopant effects by comparing the dopants that affect GF showed that Ru is the best dopant [67]. Additionally, first-principles calculations found a large piezoresistive coefficient for p-type silicon nanowires [68] that reached absolute values greater than 3000 ($\pi = -3,550 \times 10^{-11}$ Pa^{-1}) [69]. Subsequent studies on silicon nanowires revealed that the piezoresistive coefficient can be small for certain orientations [70]. Additionally, the piezoresistance of silicon nanosheets has been reported; it was shown that ultrathin silicon nanosheets possess a higher piezoresistive coefficient than silicon nanowires, which was 343×10^{-11} Pa^{-1} [71].

As reviewed above, research on nanostructures has concentrated on nanowires because of the experimental difficulties in evaluating nanostructures including mechanical operations. Thus, the importance of first-principles calculations of nanowires will increase as the device sizes shrink to the nano-scale.

III. NUMERICAL SIMULATION APPROACHES

The numerical simulation approach introduces the piezoresistive effect in semiconductor device simulation modeling. The device simulation self-consistently solves the Poisson's equation, as well as the electron and hole current equations of continuity [72]. The piezoresistive effect is introduced by modifying the mobilities of charge carriers according to the stress effects [73]. The mechanical stress is generally modeled using the finite-element method [74], which is an advancement from the conventional finite-differential method, to reduce the calculation volume and computational cost.

A. SOFTWARE

Device simulation facilitates the design of piezoresistors or devices under stress. The devices under stress include the MOSFET with strained-silicon [75] and accelerometers [76]. The studies based on device simulations are strictly limited as described above.

Sentaurus Technology-Computer-Aided-Design by Synopsys, Inc. is a commercial software package that supports mechanical and electrical simulation flow using Sentaurus Interconnect (mechanical stress simulation) and Sentaurus Device (electrical simulation) [77]. The use of this software can facilitate the design of common piezoresistors. Additionally, COMSOL Multiphysics [78] and ANSYS [79] are mechanical stress simulators. These software packages can be used for simulation modeling using the finite-element method [80]. Furthermore, device simulation includes two aspects, namely, mechanical stress and electrical simulations, and because these simulations are in separate fields, the connection between them is important. First, mechanical stress simulation is performed to obtain the stress profiles; the stresses in the longitudinal and transverse directions are necessary to evaluate the piezoresistive effect. Additionally, the strain and von-Mises stress profiles are obtained as supplementary data. Second, electrical simulation is performed to evaluate the piezoresistive effect using the stress profiles as inputs. Electrical simulation requires a corresponding model. The simplest is the piezoresistor simulation that requires only the coefficients specifying the piezoresistive effect, whereas other devices such as strained-MOSFETs require fundamental transistor modeling.

However, the simulations themselves are simple. Figure 3 illustrates the basic simulation flow for studies of piezoresistors. To simulate piezoresistance, the fundamental material parameters of semiconductor device simulation, such as the band-gap energy E_G and non-stressed mobility μ_0, are used. The unique features of piezoresistance are the mobility enhancement and the band-gap energy deformation by the stress profile as well as mobility validation from the non-stressed mobility μ_0 to the updated stressed

mobility μ_{Piezo} [34]. The band-gap energy deformation can be expressed using the effective density-of-state (DOS) derived from the effective masses and finally affects the intrinsic carrier concentration [32]. Generally, the common phenomena in semiconductors, such as carrier generation and recombination, are considered to be negligible during piezoresistor simulations. Notably, the material parameters are considered to be anisotropic, and the crystal plane or the orientation is considered to be an important factor. The minimal inputs are the piezoresistive coefficient π for the electrical part and the Young's modulus E and Poisson's ratio γ for the mechanical part. Furthermore, π expresses the resistivity change under the mechanical stress profile generated using E and γ. When the temperature effect is included, the thermal expansion coefficient α_T is added. Our previous study focused on common materials, included the temperature effect, and summarized the parameter sets [32].

A model coupling mechanical and electrical-thermal solvers was used to study of the reliability of lithium-ion battery cells [81]. Even though applications are different, the proposed model is considered to be suitable for piezoresistance applications. However, in the autho 's' opinion, because the current density of piezoresistors is much smaller than that of battery cells, the effects of self-heating that gives rise to thermal stresses are negligible for most conditions. While the sequential simulation method illustrated in Fig. 4 is sufficiently accurate for simulating piezoresistive devices such as sensors, theoretical studies of stressed MOSFETs may require the use of coupled mechanical and electrical-thermal simulations.

A simulation of MOSFET devices under the mechanical stress has been reported. Because MOSFET operations occur at the surface of the substrate, it is necessary to estimate surface stress profiles. Different piezoresistive coefficients for the bulk region and the inversion layer inside MOSFETs have been reported [82]. Evaluating the MOSFET operations under stressed conditions requires stresses in the longitudinal, transverse, and shear directions. The MOSFET length and width are useful for obtaining the surface stresses,. Using the surface stresses in the longitudinal, transverse, and shear directions, current changes can be simply expressed [82], [83].

Currently, device modeling of the piezoresistive phenomenon is mostly limited to cubic crystal systems. This is most likely due to the difficulty in determining the large number of tensor components of hexagonal crystals that makes it difficult to reproduce this phenomenon.

B. PIEZORESISTANCE MODEL

The piezoresistance model forms the core of simulation modeling, and several models are available at present.

B.1. SIMPLIFIED MOBILITY ENHANCEMENT MODEL

We developed an original device simulator specifically for solving the problems associated with the piezoresistive effect for the cubic and hexagonal crystal systems [84]. We modeled the piezoresistive effect in SeMS as follows:

$$\mu_{Piezo} = \frac{C_{l,t}}{1 + \pi_l \sigma_l + \pi_t \sigma_t} \mu_0, \tag{4}$$

where $C_{l,t}$ is the correction factor [34]. This model uses longitudinal and transverse piezoresistive coefficients; therefore, it does not include all piezoresistive coefficient tensor components in the calculations and drastically decreases the number of input parameters. This model is based on the mobility enhancement theory [85] of the piezoresistive effect.

Additionally, the temperature effect has an important effect on piezoresistance. We reported that a piezoresistive coefficient can be expressed using the ionization energy of the dopant at a high temperature [32] as follows:

$$\frac{\pi}{\pi_{RT}} = \frac{E_{Si}}{E_{mat}} \left(\frac{T_{RT}}{T} \right) + 1 - \frac{E_{Si}}{E_{mat}}, \tag{5}$$

where π_{RT} is the piezoresistive coefficient at room temperature, E_{Si} and E_{mat} are the ionization energies of silicon (= 44.3 meV for boron) and the material, respectively. This theory is based on the band-transformation under stress, and this expression is beneficial for predicting the temperature dependences from the ionization energies or determining the ionization energies from the temperature responses of piezoresistors.

Low temperature is reported to cause a different phenomenon from that of the high-temperature effect, which is described for p-type 3C-SiC piezoresistors as [86]

$$\pi = \frac{m^*}{2} \exp\left(\frac{3kT}{kT_{RT}} \right), \tag{6}$$

This expression includes the thermal shrinkage of the device under low temperature, and in the shrunk condition, the temperature effect follows the exponential function and is controlled by the effective mass. Due to the low thermal energy, the ionization effect is negligible in this condition.

At room temperature, our proposed model reproduced the experimental results well for many materials, including wide band-gap materials [32], [34]. Therefore, it is recommended for single-block piezoresistor evaluations.

B.2. FIRST-ORDER MOBILITY ENHANCEMENT MODEL

The band-deformation model is the fundamental model that is closely related to the realistic physics [87]. This model is expressed as follows:

$$\frac{\Delta \rho_{ij}}{\rho} = \sum_{k,l=1}^{3} \pi_{ijkl} \sigma_{kl}. \tag{7}$$

This model describes the first-order resistivity tensor component by the sum of the product of the piezoresistive coefficients and stress components. Furthermore, this model requires the input of all piezoresistive coefficients, which are π_{11}, π_{12}, and π_{44} for cubic crystals. Analysis of p-type silicon by considering the spin–orbit coupling (referred to as spin–orbit interaction in the literature) aiming to evaluate the

piezoresistance of p-type silicon under the typical temperature range and doping concentrations has been reported in [88]. This model is suitable for evaluating common materials such as silicon and germanium under the typical conditions of intermediate temperature and doping concentrations for which the light and heavy holes are degenerate at $k = 0$ on $E - k$ space.

B.3. SECOND-ORDER MOBILITY ENHANCEMENT MODEL

The multivalley model was proposed by Herring and Vogt [89], and its piezoresistance model is known as the second-order classical expression of piezoresistance [90]. This model considers the carrier transfer between valleys and uses the first- and second-order piezoresistive coefficients for modeling. The model can be expressed as follows:

$$\frac{\Delta\rho}{\rho_i} = \sum_j \pi_{ij}\sigma_i + \sum_{j,k} \pi_{ijk}\sigma_j\sigma_k. \tag{8}$$

Based on this expression, this model is considered to be the extended version of the band-deformation model by including the second-order piezoresistive coefficients to introduce the nonlinear piezoresistance effects. Compared to the band-deformation model, this model directly describes the resistivity components. The second-order coefficients are approximated by squaring the first-order coefficients [91]. Furthermore, an alternative non-tensor expression was reported [92] and was also derived for the extended model [94].

Additionally, under the large effective piezoresistive coefficients (such as silicon in the <110> longitudinal orientation), the third-order coefficient is necessary. Therefore, the multivalley model requires several input parameters. Recently, the same author reported the nonlinearity of piezoresistance of n-type silicon using non-zero components, stress-dependent terms, and inter-valley scattering. Additionally, the authors proposed the updated piezoresistive coefficients up to the second order to describe the piezoresistive effect with high precision [93].

B.4. SIMPLIFIED K-SPACE MODEL

Researchers at Intel Corp. proposed the valence-band transformation model using the k-space description [95]. This model was based on enhancing the switching speed of P-channel metal–oxide–semiconductor (PMOS) using the strained-silicon technology [75], and the enhancement in the hole mobility was simply described. Using the split energy Δ and effective masses in the longitudinal and transverse directions, the mobility was approximated as the device-specific tensor as follows:

$$\mu = 2\mu_0 \frac{m_t m_l}{m_t + m_l} \cdot \left[\cos^2\theta\left(\frac{f_1}{m_{t1}} + \frac{f_2}{m_{l2}}\right) + \sin^2\theta\left(\frac{f_1}{m_{l1}} + \frac{f_2}{m_{t2}}\right)\right], \tag{9}$$

with

$$f_1 = \frac{1}{1 + \exp\left(-\frac{\Delta}{kT}\right)}, \tag{10}$$

$$f_2 = 1 - f_1. \tag{11}$$

Because this model corresponds to a PMOS device, the extension to NMOS [96] is necessary to apply this model to the complementary-MOS (CMOS) technology.

B.5. SUMMARY

Currently, fundamental modeling based on mobility enhancement and temperature modeling in the high- and low-temperature regimes has been achieved. Some previous models cannot be applied to hexagonal crystals that require five piezoresistive coefficients; therefore, some approximations are necessary (setting 0 values except for that in the corresponding direction). This modeling is empirical; therefore, detailed investigations of physics and phenomena should be performed in the future.

Figure 4 compares piezoresistive models for <100>- and <110>-oriented single block stressed silicon of both p- and n-type doping from 1 Pa to 1 GPa; here, the input parameters are the default values in the Sentaurus TCAD software. For p-type silicon in <100>, Intel's simplified k-space model well reproduced the theoretical GF value of 8.58 ($GF = 6.6 \times 10^{-11}\text{Pa}^{-1} \times 130\text{GPa}$). The 1st-order model over-estimated the piezoresistive effect, and the 2nd-order model failed to estimate the piezoresistive effect. Considering that the 2nd-order model's parameters are very large that they neutralize the 1st-order model's effect (under 10 MPa stress), it was concluded that the 2nd-order model's parameters must be reassessed to reproduce the piezoresistive effect. On the contrary, in <110>, all models underestimated and outputted GF values of nearly 0, whereas the theoretical GF value is 121.3 ($GF = 71.8 \times 10^{-11}\text{Pa}^{-1} \times 169\text{GPa}$). Here, a large stress of 1 GPa leads some GF values in the 2nd-order and Intel's model; therefore, it is considered that the small-stress effect is underestimated. For n-type silicon in <100>, the theoretical GF value of -133 ($GF = -102.2 \times 10^{-11}\text{Pa}^{-1} \times 130\text{GPa}$) was well reproduced by the 1st-order model, and the 2nd-order model overestimated the piezoresistive effect. The 1st- and 2nd-order conventional piezoresistive models became unstable under high-stress conditions of over 10 MPa, and the high stress ranges became unusable when using these models. Therefore, high-stress parameters must be added for accurate estimations. In <110>, the 2nd-order model well reproduced the GF values for all ranges of stress. In conclusion, each model is appropriate for certain conditions of silicon (orientation and doping type). The <110>-oriented p-type silicon is out of evaluation, and reassessment is necessary or the use of our proposed model is recommended [34].

C. APPLICATIONS

The most common application of piezoresistance simulations is the design of piezoresistors. These simulations

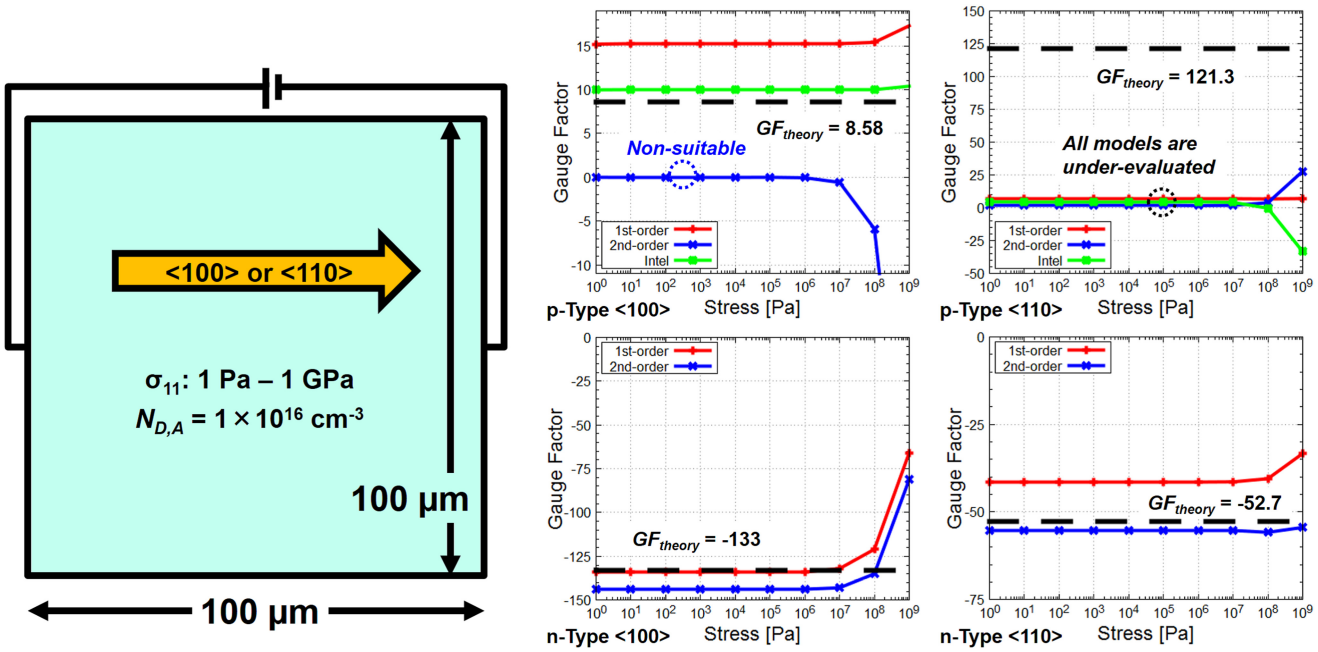

FIGURE 4. Model comparisons at p- and n-type silicons of single block piezoresistors with the different crystal orientations.

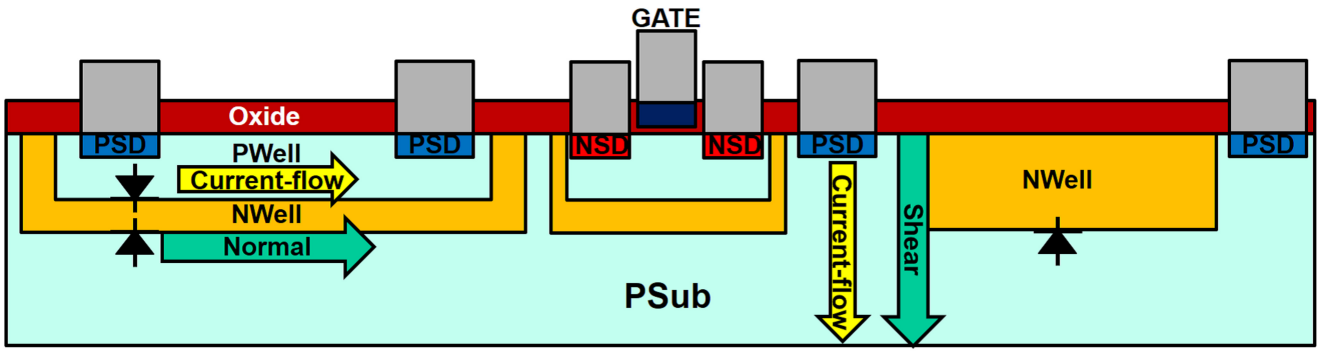

FIGURE 5. Example of integration of piezoresistive sensors on standard CMOS process chips [100].

are important for membrane structures because of their two-dimensional placement of piezoresistors as well as for the complex formation of stresses. By contrast, cantilever structures are suitable for evaluating the physics and parameters by comparing the one-dimensional effect in experiments and enabling the elimination of noise and disturbances, such as the determination of piezoresistive coefficients by reproducing the GF. Previous studies have reported the evaluation of stresses using the CMOS structure [97], [98], [99]. As illustrated in Fig. 5, a pn-junction can be used to form normal and shear stress sensors on standard CMOS chips [100] that enhance the Internet of Things (IoT) device functions.

Strained-MOSFETs will become an important component for high-speed transistors limited by shrinking process nodes [101]. Pelloux-Prayer et al. proposed empirical mobility modeling for FinFETs and fully depleted-silicon on insulator (FD-SOI) silicon transistors [102], [103]. The model includes the geometrical parameters, namely, width and height, of the nano-scale silicon channel on two 10 nm-scale transistors. Currently, the gate length of transistors has reached 1–2 nm-scale, and the quantum effect has become crucial for device operation [104]; therefore, the quantum effect is expected to be considered for the piezoresistance of such state-of-the-art transistors. Currently, germanium-based transistors are studied because of their higher carrier mobilities compared to those of silicon (approximately four-fold enhancement for electrons and two-fold enhancement for holes) [105], [106]. Furthermore, germanium possesses high piezoresistance, and the development of germanium-based strained-transistors is attractive for further advances in complementary metal oxide semiconductor technologies.

IV. FUTURE PERSPECTIVES AND OPPORTUNITIES

As demonstrated in this review, piezoresistance is still an under-researched field; however, new materials such as wide

band-gap semiconductors, nanowires, and flexible materials have been identified. For evaluating piezoresistance in wide band-gap semiconductors, the corresponding piezoresistive coefficients must be determined, and as summarized in Table 1, many values are still unavailable. This indicates that fundamental experiments on piezoresistors under several crystal orientations must be conducted. These materials are expected to be less sensitive than silicon and germanium that yield large piezoresistive effects; therefore, the applications of these materials will be limited to severe environments with high temperatures or stresses.

Most theoretical research on nanowires is based on first-principle calculations, and expansion to device simulation modeling is expected, as this will improve the design of nano-scale devices, including nano-electromechanical systems (NEMS). Its substantially large piezoresistance is attractive and nano-wires made of wide band-gap materials may support their small piezoresistance. Most research targets silicon nano-wires; however, silicon carbide, gallium nitride, and other wide band-gap materials should also be investigated. As nanowires yield large piezoresistance, highly sensitive mechanical sensors must be realized that can be implemented in standalone IoT devices.

New applications of piezoresistance are a focus in the field of flexible electronics. Zheng et al. proposed a portable bio-signal sensing device based on MXene ($Ti_3C_2T_x$)-coated nonwoven fabrics that produces piezoresistance [107]. MXene is the category of transition metal carbides that has a graphene-like sheet structure [108], and both can be used in several bio-compatible applications such as bio-signal sensing, drug delivery, and tissue engineering. Therefore, the piezoresistive function is necessary for -expansion [109]. Furthermore, MXene has the potential to exhibit certain material parameters according to the selection of the transition metal compounds [110], and MXene can be used to realize highly sensitive flexible sensors.

V. CONCLUSION

We reviewed semiconductor piezoresistance in terms of numerical simulations, material properties, and device simulations. The important fundamental parameters were listed, and the major piezoresistance models useful for these simulations were introduced. Finally, the applications of piezoresistance simulations were discussed in association with the material properties, physics, and development of high-end devices.

REFERENCES

[1] A. A. Barlian, W. Park, J. R. Mallon Jr., A. J. Rastegar, and B. L. Pruitt, "Review: semiconductor piezoresistance for microsystems," *Proc. IEEE*, vol. 97, no. 3, pp. 513–552, Mar. 2009. [Online]. Available: https://doi.org/10.1109/JPROC.2009.2013612

[2] A. S. Algamili et al., "A review of actuation and sensing mechanisms in MEMS-based sensor devices," *Nanoscale Res. Lett.*, vol. 16, p. 16, Jan. 2021. [Online]. Available: https://doi.org/10.1186/s11671–021-03481–7

[3] R. Hajare, V. Reddy, and R. Srikanth, "MEMS based sensors–A comprehensive review of commonly used fabrication techniques," *Mater. Today Proc.*, vol. 49, part 3, pp. 720–730, May 2021. [Online]. Available: https://doi.org/10.1016/j.matpr.2021.05.223

[4] A. A. M. Faudzi, Y. Sabzehmeidani, and K. Suzumori, "Application of micro-electro-mechanical systems (MEMS) as sensors: A review," *J. Robot. Mechatron.*, vol. 32, no. 2, pp. 281–288, Apr. 2020. [Online]. Available: https://doi.org/10.20965/jrm.2020.p0281

[5] J. C. Doll and B. L. Pruitt, "Piezoresistor design and applications," in *Microsystems and Nanosystems*. New York, NY, USA: Springer, 2013. [Online]. Available: https://doi.org/10.1007/978–1-4614–8517-9

[6] M. Lades, J. Frank, J. Funk, and G. Wachutka, "Analysis of piezoresistive effects in silicon structures using multidimensional process and device simulation," in *Simulation of Semiconductor Devices and Processes*. Vienna, Austria: Springer, 1995, pp. 22–25. [Online]. Available: https://doi.org/10.1007/978–3-7091–6619-2_5

[7] H. Phan, D. V. Dao, K. Nakamura, S. Dimitrijev, and N. Nguyen, "The piezoresistive effect of SiC for MEMS sensors at high temperatures: A review," *J. Microelectromech. Syst.*, vol. 24, no. 6, pp. 1663–1677, Dec. 2015. [Online]. Available: https://doi.org/10.1109/JMEMS.2015.2470132

[8] L. E. Hollander, G. L. Vick, and T. J. Diesel, "The piezoresistive effect and its applications," *Rev. Sci. Instrum.*, vol. 31, no. 3, pp. 323–327, Mar. 1960. [Online]. Available: https://doi.org/10.1063/1.1716967

[9] J. N. Burghartz, *Ultra-Thin Chip Technology And Applications*. New York, NY, USA: Springer, Nov. 2010. [Online]. Available: https://doi.org/10.1007/978–1-4419–7276-7_19

[10] A. S. Fiorillo, C. D. Critello, and S. A. Pullano, "Theory, technology and applications of piezoresistive sensors: A review," *Sens. Actuator A, Phys.*, vol. 281, pp. 156–175, Oct. 2018. [Online]. Available: https://doi.org/10.1016/j.sna.2018.07.006

[11] W. G. Pann, and R. N. Thurston, "Semiconducting stress transducers utilizing the transverse and shear piezoresistance effects," *J. Appl. Phys.*, vol. 32, no. 10, pp. 2008–2019, Oct. 1961. [Online]. Available: https://doi.org/10.1063/1.1728280

[12] M. A. Hopcroft, W. D. Nix, and T. W. Kenny, "What is the Young's modulus of silicon?" *J. Microelectromech. Syst.*, vol. 19, no. 2, pp. 229–238, Apr. 2010. [Online]. Available: https://doi.org/10.1109/JMEMS.2009.2039697

[13] K. Matsumoto and I. Shimoyama, "MEMS sensor devices with a piezo-resistive cantilever," *Int. J. Autom. Technol.*, vol. 12, no. 1, pp. 4–14, Jan. 2018. [Online]. Available: https://doi.org/10.20965/ijat.2018.p0004

[14] Z. Huang and X. Ma, "An improvement of membrane structure of MEMS piezoresistive pressure sensor," in *Proc. 16th Int. Conf. Electron. Packaging Technol. (ICEPT)*, Aug. 2015, pp. 1174–1179. [Online]. Available: https://doi.org/10.1109/ICEPT.2015.7236789

[15] F. Loizeau, T. Akiyama, S. Gautsch, P. Vettiger, G. Yoshikawa, and N. F. de Rooij, "Comparing membrane- and cantilever-based surface stress sensors for reproducibility," *Sens. Actuators A, Phys.*, vol. 228, pp. 9–15, Jun. 2015. [Online]. Available: https://doi.org/10.1016/j.sna.2015.02.039

[16] C. S. Smith, "Piezoresistance effect in germanium and silicon," *Phys. Rev. B, Condens. Matter*, vol. 94, no. 1, pp. 42–49, Apr. 1954. [Online]. Available: https://doi.org/10.1103/PhysRev.94.42

[17] J. Barden, and W. Schokley, "Deformation potentials and mobilities in non-polar crystals," *Phys. Rev.*, vol. 80, pp. 72–80, Oct. 1950. [Online]. Available: https://doi.org/10.1103/PhysRev.80.72

[18] J. Richter, J. Pedersen, M. Brandbyge, E. V. Thomsen, and O. Hansen, "Piezoresistance in p-type silicon revisited," *J. Appl. Phys.*, Vol. 104, no. 2, Jul. 2008, Art. no. 23715. [Online]. Available: https://doi.org/10.1063/1.2960335

[19] K. Matsuda, S. Nagaoka, and H. Kajiyama, "Origin of the piezoresistance effects in *p*-type silicon at high temperature," *Jpn. J. Appl. Phys.*, vol. 58, no. 9, Aug. 2019, Art. no. 98002. [Online]. Available: https://doi.org/10.7567/1347–4065/ab3559

[20] Y. Kanda and K. Matsuda, "Piezoresistance effect of n-type silicon; temperature and concentration dependencies, stress dependent effective masses," *AIP Conf. Proc.*, vol. 893, no. 1, pp. 173–174, May 2007. [Online]. Available: https://doi.org/10.1063/1.2729825

[21] K. Matsuda, S. Nagaoka, and Y. Kanda, "Graphical representation and origin of piezoresistance effect in germanium," *J. Phys. Conf. Series*, vol. 864, Jun. 2017, Art. no. 12045. [Online]. Available: https://doi.org/10.1088/1742–6596/864/1/012045

[22] K. Matsuda, S. Nagaoka, and H. Kajiyama, "Origin of the piezoresistance effects in p-type silicon at high temperature," *Jpn. J. Appl. Phys.*, vol. 58, no. 9, Aug. 2019, Art. no. 98002. [Online]. Available: https://doi.org/10.7567/1347–4065/ab3559

[23] H.-P. Phan et al., "Piezoresistive effect of p-type single crystalline 3C-SiC thin film," *IEEE Electron Device Lett.*, vol. 35, no. 3, pp. 399–401, Mar. 2014. [Online]. Available: https://doi.org/10.1109/LED.2014.2301673

[24] H.-P. Phan et al., "Fundamental piezoresistive coefficients of p-type single crystalline 3C-SiC," *Appl. Phys. Lett.*, vol. 104, no. 11, Mar. 2014, Art. no. 111905. [Online]. Available: https://doi.org/10.1063/1.4869151

[25] J. S. Shor, D. Goldstein, and A. D. Kurtz, "Characterization of n-type β-SiC as a piezoresistor," *IEEE Trans. Electron Devices*, vol. 40, no. 6, pp. 1093–1099, Jun. 1993. [Online]. Available: https://doi.org/10.1109/16.214734

[26] H.-P. Phan et al., "Characterization of the piezoresistance in highly doped p-type 3C-SiC at cryogenic temperatures," *RSC Adv.*, vol. 8, no. 52, pp. 29976–29979, Aug. 2018. [Online]. Available: https://doi.org/10.1039/c8ra05797d

[27] H.-P. Phan et al., "Piezoresistive effect in p-type 3C-SiC at high temperatures characterized using Joule heating," *Sci. Rep.*, vol. 6, Jun. 2016, Art. no. 28499. [Online]. Available: https://doi.org/10.1038/srep28499

[28] T. Nguyen et al., "Isotropic piezoresistance of p-type 4H-SiC in (0001) plane," *Appl. Phys. Lett.* vol. 113, no. 1, Jul. 2018, Art. no. 12104. [Online]. Available: https://doi.org/10.1063/1.5037545

[29] B. Tian, H. Shang, D. Wang, Y. Liu, and W. Wang, "Investigation of piezoresistive effect of n-type 4H-SiC based on all-SiC pressure sensors," *IEEE Sens. J.*, vol. 22, no. 7, pp. 6435–6441, Apr. 2022. [Online]. Available: https://doi.org/10.1109/JSEN.2022.3153630

[30] T. Nguyen, H. Phan, T. Dinh, A. R. M. Foisal, N. Nguyen, and D. V. Dao, "High-temperature tolerance of the piezoresistive effect in p-4H-SiC for harsh environment sensing," *J. Mater. Chem. C*, vol. 6, no. 32, pp. 8613–8617, Jul. 2018. [Online]. Available: https://doi.org/10.1039/C8TC03094D

[31] J. S. Shor, L. Bemis, and A. D. Kurtz, "Characterization of monolithic n-type 6H-SiC piezoresistive sensing elements," *IEEE Trans. Electron Devices*, vol. 41, no. 5, pp. 661–665, May 1994. [Online]. Available: https://doi.org/10.1109/16.285013

[32] T. Sugiura, N. Takahashi, R. Sakota, K. Matsuda, and N. Nakano, "High-temperature piezoresistance of silicon carbide and gallium nitride materials," *IEEE J. Electron Devices Soc.*, vol. 10, pp. 203–211, Feb. 2022. [Online]. Available: https://doi.org/10.1109/JEDS.2022.3150915

[33] T. Toriyama, "Piezoresistance consideration on n-type 6H SiC for MEMS-based piezoresistance sensors," *J. Micromech. Microengineer.* vol. 14, no. 11, pp. 1445–1448, Aug. 2004. [Online]. Available: https://doi.org/10.1088/0960–1317/14/11/002

[34] T. Sugiura, N. Takahashi, and N. Nakano, "The piezoresistive mobility modeling for cubic and hexagonal silicon carbide crystals," *J. Appl. Phys.*, vol. 127, no. 24, Jun. 2020, Art. no. 245113. [Online]. Available: https://doi.org/10.1063/5.0006830

[35] J. G. Gualtieri, J. A. Kosinski, and A. Ballato, "Piezoelectric materials for acoustic wave applications," *IEEE Trans. Ultrason., Ferroelect., Freq. Control*, vol. 41, no. 1, pp. 53–59, Jan. 1994. [Online]. Available: https://doi.org/10.1109/58.265820

[36] A. D. Bykhovski, V. V. Kaminski, M. S. Shur, Q. C. Chen, and M. A. Khan, "Piezoresistive effect in wurtzite n-type GaN," *Appl. Phys. Lett.*, vol. 68, no. 6, pp. 818–819, Feb. 1996. [Online]. Available: https://doi.org/10.1063/1.116543

[37] V. Tilak, A. Vertiatchikh, J. Jiang, N. Reeves, and S. Dasgupta, "Piezoresistive and piezoelectric effects in GaN," *Physica Status Solidi C, Appl. Res.*, vol. 3, no. 6, pp. 2307–2311, Jun. 2006. [Online]. Available: https://doi.org/10.1002/pssc.200565217

[38] Y. Lin, S. Huang, M. Houng, Y. Hsieh, Y. Juang, and J. V. Li, "Piezoresistive effect and strain gauge application of β-Ga_2O_3," *Jpn. J. Appl. Phys.*, vol. 58, no. 11, Oct. 2019, Art. no. 111003. [Online]. Available: https://doi.org/10.7567/1347–4065/ab4c9c

[39] N. Takahashi, T. Sugiura, R. Sakota, and N. Nakano, "Numerical simulation of the piezoresistive effect of βGa_2O_3 in the <010> direction," *Jpn. J. Appl. Phys.*, vol. 60, Mar. 2021, Art. no. SCCL05. [Online]. Available: https://doi.org/10.35848/1347–4065/abe7ff

[40] M. A. Fraga, H. Furlan, R. S. Pessoa, L. A. Rasia, and C. F. R. Mateus, "Studies on SiC, DLC and TiO_2 thin films as piezoresistive sensor materials for high temperature application," *Microsyst. Technol.*, vol. 18, pp. 1027–1033, Jan. 2012. [Online]. Available: https://doi.org/10.1007/s00542–012-1435-y

[41] A. Dehé, K. Fricke, K. Mutamba, and H. L. Hartnagel, "A piezoresistive GaAs pressure sensor with GaAs/AlGaAs membrane technology," *J. Micromech. Microeng.*, vol. 5, no. 2, pp. 139–142, 1995. [Online]. Available: https://doi.org/10.1088/0960–1317/5/2/021

[42] A. Ferreira, J. P. Silva, R. Rodrigues, N. Martin, S. Lanceros-Méndez, and F. Vaz, "High performance piezoresistive response of nanostructured ZnO/Ag thin films for pressure sensing applications," *Thin Solid Films*, vol. 691, Dec. 2019, Art. no. 137587. [Online]. Available: https://doi.org/10.1016/j.tsf.2019.137587

[43] K. Takenaka, H. Umezawa, S. Kato, A. Chayahara, and S. Shikata, "Crystal orientation dependence of piezoresistivity in boron doped single crystalline diamond films," *Diamond Relat. Mater.*, vol. 63, pp. 218–221, Mar. 2016. [Online]. Available: https://doi.org/10.1016/j.diamond.2015.09.005

[44] M. Werner, P. Glunche, M. Adamschik, E. Kohn, and H. Fecht, "Review on diamond based piezoresistive sensors," in *Proc. IEEE Inter. Symp. Ind. Electron. (ISIE)*, Jul. 1998, pp. 147–152. [Online]. Available: https://doi.org/10.1109/ISIE.1998.707766

[45] R. He and P. Yang, "Giant piezoresistance effect in silicon nanowires," *Nat. Nanotech.*, vol. 1, pp. 42–46, Oct. 2006. [Online]. Available: https://doi.org/10.1038/nnano.2006.53

[46] L. Wang et al., "Improved piezoresistive properties of ZnO/SiC nanowire heterojunctions with an optimized piezoelectric nanolayer," *J. Mater. Sci.*, vol. 56, pp. 17146–17155, Aug. 2021. [Online]. Available: https://doi.org/10.1007/s10853–021-06411–1

[47] E. Fakhri et al., "Piezoresistance characterization of silicon nanowires in uniaxial and isostatic pressure variation," *Sensors*, vol. 22, no. 17, p. 6340, Aug. 2022. [Online]. Available: https://doi.org/10.3390/s22176340

[48] A. C. H. Rowe, "Piezoresistance in silicon and its nanostructures," *J. Mater. Res.*, vol. 29, no. 6, pp. 731–744, Mar. 2014. [Online]. Available: https://doi.org/10.1557/jmr.2014.52

[49] T. Barwicz, L. Klein, S. J. Koester, and H. Hamann, "Silicon nanowire piezoresistance: Impact of surface crystallographic orientation," *Appl. Phys. Lett.* vol. 97, no. 2, Jul. 2010, Art. no. 23110. [Online]. Available: https://doi.org/10.1063/1.3463456

[50] L. Lou et al., "Characteristics of NEMS piezoresistive silicon nanowires pressure sensors with various diaphragm layers," *Procedia Eng.*, vol. 25, pp. 1433–1436, Dec. 2011. [Online]. Available: https://doi.org/10.1016/j.proeng.2011.12.354

[51] C. Ti et al., "Optimization of piezoresistive motion detection for ambient NEMS applications," in *Proc. IEEE Sens.*, Oct. 2020, pp. 1–4. [Online]. Available: https://doi.org/10.1109/SENSORS47125.2020.9278593

[52] X. Li et al., "A giant negative piezoresistance effect in 3C-SiC nanowires with B dopants," *J. Mater. Chem.*, vol. 4, no. 27, pp. 6466–6472, Jun. 2016. [Online]. Available: https://doi.org/10.1039/C6TC01882C

[53] J. Li, L. Fang, B. Sun, X. Li, and S. H. Kang, "Review—Recent progress in flexible and stretchable piezoresistive sensors and their applications," *J. Electrochem. Soc.* vol. 167, no. 3, Feb. 2020, Art. no. 37561. [Online]. Available: https://doi.org/10.1149/1945–7111/ab6828

[54] C. So et al., "Epidermal piezoresistive structure with deep learning-assisted data translation," *NPJ Flexible Electrons*. vol. 6, p. 70, Aug. 2022. [Online]. Available: https://doi.org/10.1038/s41528–022-00200–9

[55] F. S. Irani et al., "Graphene as a piezoresistive material in strain sensing applications," Micromach. vol. 13, no. 1, p. 119, Jan. 2022. [Online]. Available: https://doi.org/10.3390/mi13010119

[56] E. Ricohermoso III et al., "Piezoresistive carbon-containing ceramic nanocomposites–A review," *Open Ceramics* vol. 5, Mar. 2021, Art. no. 100057. [Online]. Available: https://doi.org/10.1016/j.oceram.2021.100057

[57] M. S. Cetin and H. A. K. Toprakci, "Flexible electronics from hybrid nanocomposites and their application as piezoresistive strain sensors," *Composite Part B, Eng.*, vol. 224, Nov. 2021, Art. no. 109199. [Online]. Available: https://doi.org/10.1016/j.compositesb.2021.109199

[58] R. Nandee, M. A. Chowdhury, A. Shahid, N. Hossain, and M. Rana, "Band gap formation of 2D materialin graphene: Future prospect and challenges," *Results Eng.*, vol. 15, Sep. 2022, Art. no. 100474. [Online]. Available: https://doi.org/10.1016/j.rineng.2022.100474

[59] A. Chaves et al., "Bandgap engineering of two-dimensional semiconductor materials," *NPJ 2D Mater. Appl.*, vol. 4, p. 29, Aug. 2020. https://doi.org/10.1038/s41699–020-00162–4

[60] R. Hegde, K. Ramji, and P. Swapna, "Simulation of carbon nanotubes polymer based piezoresistive flexible pressure sensor for ultra sensitive electronic skin," in *Proc. 2nd Int. Conf. Electron. Mater. Eng. Nano-Technol. (IEMENTech)*, May 2018. [Online]. Available: https://doi.org/10.1109/IEMENTECH.2018.8465202

[61] A. Vilouras, H. Heidari, S. Gupta, and R. Dahiya, "Modeling of CMOS devices and circuits on flexible ultrathin chips," *IEEE Trans. Electron Devices*, vol. 64, no. 5, pp. 2038–2046, May 2017. [Online]. Available: https://doi.org/10.1109/TED.2017.2668899

[62] J. Kestyn and E. Polizzi, "From fundamental first-principle calculations to nanoengineering applications: A review of the NESSIE project," *IEEE Nanotechnol. Mag.*, vol. 14, no. 6, pp. 52–68, Dec. 2020. [Online]. Available: https://doi.org/10.1109/MNANO.2020.3024387

[63] S. Smidstrup et al., "QuantumATK: An integrated platform of electronic and atomic-scale modelling tools," *J. Phys. Condens. Matter* vol. 32, no. 1, Nov. 2019, Art. no. 15901. [Online]. Available: https://doi.org/10.1088/1361–648X/ab4007

[64] "Welcome to Python.org." Accessed: Jun. 8, 2023. [Online]. Available: https://www.python.org/

[65] K. Nakamura, Y. Isono, T. Toriyama, and S. Sugiyama, "Simulation of piezoresistivitiy in *n*-type single-crystal silicon on the basis of the first-principles band structure," *Phys. Rev. B, Condens. Matter*, vol. 80, no. 4, Jul. 2009, Art. no. 45205. [Online]. Available: https://doi.org/10.1103/PhysRevB.80.045205

[66] F. H. Pollak and M. Cardona, "Piezo-electroreflectance in Ge, GaAs, and Si," *Phys. Rev.*, vol. 172, no. 3, pp. 816–837, Aug. 1968. [Online]. Available: https://doi.org/10.1103/PhysRev.172.816

[67] C. T. Ser, A. M. Mak, T. Wejrzanowski, and T. L. Tan, "Designing piezoresistive materials from first-principles: Dopant effects on 3C-SiC," *Comput. Mater. Sci.*, vol. 186, Jan. 2021, Art. no. 110040. [Online]. Available: https://doi.org/10.1016/j.commatsci.2020.110040

[68] K. Nakamura, Y. Isono, and T. Toriyama, "First-principles study on piezoresistance effect in silicon nanowires," *Jpn. J. Appl. Phys.*, vol. 47, no. 6S, pp. 5132–5138, Jun. 2008. [Online]. Available: https://doi.org/10.1143/JJAP.47.5132

[69] J. X. Cao, X. G. Gong, and R. Q. Wu, "Giant piezoresistance and its origin in Si(111) nanowires: First-principles calculations," *Phys. Rev. B, Condens. Matter*, vol. 75, Apr. 2007, Art. no. 233302. [Online]. Available: https://doi.org/10.1103/PhysRevB.75.233302

[70] K. Nakamura, Y. Isono, T. Toriyama, and S. Sugiyama, "First-principles simulation on orientation dependence of piezoresistance properties in silicon nanowires," *Jpn. J. Appl. Phys.*, Vol. 48, no. 6S, Jun. 2009, Art. no. 06FG09. [Online]. Available: https://doi.org/10.1143/JJAP.48.06FG09

[71] K. Nakamura, T. Toriyama, and S. Sugiyama, "First-principles simulation on piezoresistive properties in doped silicon nanosheets," *IEEJ Trans. Electr. Electron. Eng.*, vol. 5, no. 2, pp. 157–163, Mar. 2010. [Online]. Available: https://doi.org/10.1002/tee.20511

[72] W. Fichtner, D. J. Rose, and R. E. Bank, "Semiconductor device simulation," *IEEE Trans. Electron Devices*, vol. ED-30, no. 9, pp. 1018–1030, Sep. 1983. [Online]. Available: https://doi.org/10.1109/T-ED.1983.21256

[73] M. Koganemaru, T. Ikeda, N. Miyazaki, and H. Tomokage, "Experimental and numerical evaluation of stress effects on DC characteristics of nMOSFETs," *IEICE Trans. Electron. C*, vol. 90, no. 4, pp. 351–362, Apr. 2007.

[74] M. J. Turner, R. W. Clough, H. C. Martin, and L. J. Topp, "Stiffness and deflection analysis of complex structures," *J. Aeronautical Sci.*, vol. 23, no. 9, pp. 805–854, Sep. 1956. [Online]. Available: https://doi.org/10.2514/8.3664

[75] S. C. Thompson et al., "A logic nanotechnology featuring strained-silicon," *IEEE Electron Device Lett.*, vol. 25, no. 4, pp. 191–193, Apr. 2004. [Online]. Available: https://doi.org/10.1109/LED.2004.825195

[76] A. Béliveau, G. T. Spencer, K. A. Thomas, and S. L. Roberson, "Evaluation of MEMS capacitive accelerometers," *IEEE Des. Test Comput.*, vol. 16, no. 4, pp. 48–56, Oct./Dec. 1999. [Online]. Available: https://doi.org/10.1109/54.808209

[77] P. Pfäffli et al., "TCAD modeling for reliability," *Microelectron. Reliabil.* vols. 88–90, pp. 1083–1089, Sep. 2018. [Online]. Available: https://doi.org/10.1016/j.microrel.2018.06.109

[78] R. S. Jakati, K. B. Balavalad, and B. G. Sheeparamatti, "Comparative analysis of different micro-pressure sensors using COMSOL multiphysics," in *Proc. Int. Conf. Elect., Electr. Commun. Comput. Opt. Techn. (ICEECCOT)*, Dec. 2016, pp. 355–360. [Online]. Available: https://doi.org/10.1109/ICEECCOT.2016.7955245

[79] Y. Sahi, S. Sharma, and S. Chandan, "Design of piezoresistive sensor using FEA in ANSYS," *IOP Conf. Series Mater. Sci. Eng.* vol. 748, Feb. 2020, Art. no. 12011. [Online]. Available: https://doi.org/10.1088/1757–899X/748/1/012011

[80] M. Pustan, S. Paquay, V. Rochusm, and J. Golinval, "Modeling and finite element analysis of mechanical behavior of flexible MEMS components," *Microsyst. Technol.*, vol. 17, pp. 553–562, Feb. 2011. [Online]. Available: https://doi.org/10.1007/s00542–011-1232-z

[81] C. Zhang, S. Santhanagopalan, M. A. Sprague, and A. A. Pesaran, "A representative-sandwich model for simultaneously coupled mechanical-electrical-thermal simulation of a lithium-ion cell under quasi-static indentation tests," *J. Power Sources*, vol. 298, pp. 309–321, Dec. 2015. [Online]. Available: https://doi.org/10.1016/j.jpowsour.2015.08.049

[82] B. Sbierski, P. Gieschke, and O. Paul, "Shear piezoresistance in MOSFET devices under general operating conditions," *IEEE Trans. Electron Devices*, vol. 58, no. 12, pp. 4145–4154, Dec. 2011. [Online]. Available: https://doi.org/10.1109/TED.2011.2166556

[83] R. C. Jaeger, J. C. Suhling, R. Ramani, A. T. Bradley, and J. Xu, "CMOS stress sensors on (100) silicon," *IEEE J. Solid-State Circuits*, vol. 35, no. 1, pp. 85–95, Jan. 2000. [Online]. Available: https://doi.org/10.1109/4.818923

[84] T. Sugiura, N. Takahashi, and N. Nakano, "Evaluation of p-type 4H-SiC piezoresisitance coefficients in (0001) plane using numerical simulation," *Mater. Sci. Forum*, vol. 1004, pp. 249–255, Jul. 2020. [Online]. Available: https://doi.org/10.4028/www.scientific.net/MSF.1004.249

[85] K. Uchida, T. Krishnamohan, K. C. Saraswat, and Y. Nishi, "Physical mechanisms of electron mobility enhancement in uniaxial stressed MOSFETs and impact of uniaxial stress engineering in ballistic regime," in *IEEE Int. Elect. Dev. Meeting (IEDM) Tech. Dig.*, Dec. 2005. https://doi.org/10.1109/IEDM.2005.1609286

[86] T. Sugiura, N. Takahashi, R. Sakota, K. Matsuda, and N. Nakano, "Piezoresistive thermal characteristics of aluminum-doped p-type 3C-silicon carbides," *IEEE J. Electron Devices Soc.*, vol. 10, pp. 547–553, 2022. [Online]. Available: https://doi.org/10.1109/JEDS.2022.3191543

[87] T. Manku and A. Nathan, "Valence energy-band structure for strained group-IV semiconductors," *J. Appl. Phys.*, vol. 73, no. 3, pp. 1205–1213, Feb. 1993. [Online]. Available: https://doi.org/10.1063/1.353287

[88] T. Toriyama and S. Sugiyama, "Analysis of piezoresistance in p-type silicon for mechanical sensors," *J. Microelectromech. Syst.*, vol. 11, no. 5, pp. 598–604, Oct. 2002. [Online]. Available: https://doi.org/10.1109/JMEMS.2002.802904

[89] C. Herring and E. Vogt, "Transport and deformation-potential theory for many-valley semiconductors with anisotropic scattering," *Phys. Rev.*, vol. 101, no. 3, pp. 944–961, Feb. 1956. [Online]. Available: https://doi.org/10.1103/PhysRev.101.944

[90] K. Matsuda, Y. Kanda, K. Yamamura, and K. Suzuki, "Nonlinearity of piezoresistance effect in p- and n-type silicon," *Sens. Actuator A Phys.*, vol. 21, nos. 1–3, pp. 45–48, Feb. 1990. [Online]. Available: https://doi.org/10.1016/0924-4247(90)85008-R

[91] K. Suzuki, H. Hasegawa, and Y. Kanda, "Origin of the linear and nonlinear piezoresistance effects in p-type silicon," *Jpn. J. Appl. Phys.*, vol. 23, no. 11A, pp. L871–L874, Nov. 1984. [Online]. Available: https://doi.org/10.1143/JJAP.23.L871

[92] J. T. Lenkkeri, "Nonlinear effects in the piezoresistivity of p-type silicon," *Phys. Status Solidi B*, vol. 186, no. 1, pp. 373–385, Jul. 1986. [Online]. Available: https://doi.org/10.1002/pssb.2221360141
[93] K. Matsuda, H. Uyama, and K. Tsutsui, "Nonlinear piezoresistance coefficients of semiconductors," *J. Appl. Phys.*, vol. 126, no. 22, Dec. 2019, Art. no. 225701. [Online]. Available: https://doi.org/10.1063/1.5121884
[94] K. Matsuda, K. Suzuki, K. Yamamura, and Y. Kanda, "Nonlinear piezoresistance effects in silicon," *J. Appl. Phys.*, vol. 73, no. 4, pp. 1838–1847, Feb. 1993. [Online]. Available: https://doi.org/10.1063/1.353169
[95] B. Obradovic et al., "A physically-based analytic model for stress-induced hole mobility enhancement," *J. Comput. Electron.*, vol. 3, pp. 161–164, Oct. 2004. [Online]. Available: https://doi.org/10.1007/s10825–004-7037-x
[96] Q. Xiang, J. Goo, J. Pan, B. Yu, S. Ahmed, J. Zhang, and M. Lin, "Strained silicon NMOS with nickel-silicide metal gate," in *Symp. VLSI Tech. Dig. Tech. Papers*, Aug. 2003, pp. 101–102. [Online]. Available: https://doi.org/10.1109/VLSIT.2003.1221106
[97] T. Sugiura, H. Miura, and N. Nakano, "High-temperature operational piezoresistive pressure sensor on standard CMOS process," *IEEE Trans. Circuits Syst. II, Exp. Briefs*, vol. 70, no. 2, pp. 726–730, Feb. 2023. [Online]. Available: https://doi.org/10.1109/TCSII.2022.3213580
[98] M. Baumann, B. Lemke, P. Ruther, and O. Paul, "Piezoresistive CMOS sensors for out-of-plane shear stress," in *Proc. IEEE SENSORS*, Oct. 2009, pp. 441–444. [Online]. Available: https://doi.org/10.1109/ICSENS.2009.5398265
[99] B. Lemke, M. Baumann, P. Giescheke, R. Baskaran, and O. Paul, "Piezoresistive CMOS-compatible sensor for out-of-plane shear stress," *Sens. Actuators A, Phys.*, vol. 189, pp. 488–495, Jan. 2013. [Online]. Available: https://doi.org/10.1016/j.sna.2012.10.014
[100] T. Sugiura, K. Yamamura, Y. Watanabe, S. Yamakiri, and N. Nakano, "Circuits and devices for standalone large-scale integration (LSI) chips and Internet of Things (IoT) applications: A review," *Chip*, Apr. 2023, Art. no. 100048. [Online]. Available: https://doi.org/10.1016/j.chip.2023.100048
[101] T. N. Theis and H.-S. P. Wong, "The end of Moore's law: A new beginning for information technology," *Comput. Sci. Eng.*, vol. 19, no. 2, pp. 41–50, MAr./Apr. 2017. [Online]. Available: https://doi.org/10.1109/MCSE.2017.29
[102] J. Pelloux-Prayer et al., "Strain effect on mobility in nanowire MOSFETs down to 10 nm width: Geometrical effects and piezoresistive model," *Solid State Electron.*, vol. 125, pp. 175–181, Nov. 2016. [Online]. Available: https://doi.org/10.1016/j.sse.2016.09.002
[103] J. Pelloux-Prayer et al., "Strain effect on mobility in nanowire MOSFETs down to 10nm width: geometrical effects and piezoresistive model," in *Proc. 45th Eur. Solid State Device Res. Conf. (ESSDERC)*, Sep. 2015, pp. 210–213. [Online]. Available: https://doi.org/10.1109/ESSDERC.2015.7324752
[104] T. Sugiura, S. Yamakiri, and N. Nakano, "Germanium- and silicon-nanotransistor designs by electrical and thermal self-consistent analysis," *IEEE Trans. Comput.-Aided Design Integr. Circuits Syst.*, early access, Jan. 30, 2023, doi: 10.1109/TCAD.2023.3240938. [Online]. Available: https://doi.org/10.1109/TCAD.2023.3240938
[105] Y. Zhao, Z. Zheng, J. Li, D. Ni, and R. Zhang, "Ge CMOS technology with advanced interface and junction engineering," in *Proc. Int. Conf. IC Design Tech. (ICICDT)*, Otranto, Italy, Jun. 2018, pp. 153–156. [Online]. Available: https://doi.org/10.1109/ICICDT.2018.8399779
[106] C. S. Fuller and J. C. Severiens, "Mobility of impurity ions in germanium and silicon," *Phys. Rev.*, vol. 96, no. 1, pp. 21–25, Oct. 1954. [Online]. Available: https://doi.org/10.1103/PhysRev.96.21
[107] W. Zheng et al., "On-skin flexible pressure sensor with high sensitivity for portable pulse monitoring," *Micromachines*, vol. 13, no. 9, p. 1390, Aug. 2022. [Online]. Available: https://doi.org/10.3390/mi13091390
[108] R. Gautam, N. Marriwala, and R. Devi, "A review: study of Mxene and graphene together," *Meas. Sens.*, vol. 25, Feb. 2023, Art. no. 100592. [Online]. Available: https://doi.org/10.1016/j.measen.2022.100592
[109] E. Mostafavi and S. Iravani, "MXene-graphene composites: a perspective on biomedical potentials," *Nano-Micro Lett.*, vol. 14, p. 130, Jun. 2022. [Online]. Available: https://doi.org/10.1007/s40820–022-00880-y
[110] Y. Gogotsi and B. Anasori, "The rise of MXenes," *ACS Nano*, vol. 13, no. 8, pp. 8491–8494, Aug. 2019. [Online]. Available: https://doi.org/10.1021/acsnano.9b06394

TAKAYA SUGIURA (Member, IEEE) received the B.S., M.S., and Ph.D. degrees in electrical engineering from Keio University, Yokohama, in 2016, 2018, and 2021, respectively. His research interests include c-Si solar cells, piezoresistive devices, photonics devices, power electronics, analog LSI designs, and nanoscale transistors. He has been a member of the Electron Devices Society, Power Electronics Society, and Photonics Society since 2022.

KAZUNORI MATSUDA received the Ph.D. degree from Tsukuba University in 1993. From 2000 to 2003, he collaborated with Prof. Karl Hess's Group in UIUC for simulations on hot carriers and reliability of MOSFET. He has been a Professor with the Department of Nano Material and Bio Engineering, Tokushima Bunri University since 2022. He is currently an Invited Professor with the Division of Electrical, Electronic and Infocommunications Engineering, Graduate School of Engineering, Osaka University. He is currently working on wide-bandgap semiconductors. His research interests include transport phenomena in strained semiconductors and their applications.

NOBUHIKO NAKANO (Member, IEEE) was born in 1968. He received the B.S., M.S., and Ph.D. degrees in electrical engineering from Keio University, Japan, in 1990, 1992, and 1995, respectively, where he joined the Department of Electronics and Electrical Engineering as an Instructor in 1996. He is currently a Professor with the Faculty of Science and Technology, Department of Electronics and Electrical Engineering, Keio University and working on the design of an on-chip microsystem and biomedical LSIs. His research interests include LSI/TCAD, numerical simulations, and modeling.